Journal of Cosmetics, Dermatological Sciences and Applications, 2023, 13, 165-178
https://www.scirp.org/journal/jcdsa
ISSN Online: 2161-4512
ISSN Print: 2161-4105

A Novel Facial Cream Based on Skin Penetrable Hemp Oil Microparticles

Rachel Lubart[1,2], Inbar Yariv[3,4], Dror Fixler[3,4], Ayelet Rothstein[1], Arie Gruzman[1], Anat Lipovsky[5]

[1]Department of Chemistry, Bar Ilan University, Ramat-Gan, Israel
[2]Physics Department of Faculty of Exact Sciences, Bar Ilan University, Ramat-Gan, Israel
[3]Faculty of Engineering, Bar Ilan University, Ramat-Gan, Israel
[4]Institute of Nanotechnology and Advanced Materials, Bar-Ilan University, Ramat-Gan, Israel
[5]Hava Zingboim Ltd., Ramat-Gan, Israel
Email: ecoli2310@yahoo.com

How to cite this paper: Lubart, R., Yariv, I., Fixler, D., Rothstein, A., Gruzman, A. and Lipovsky, A. (2023) A Novel Facial Cream Based on Skin Penetrable Hemp Oil Microparticles. *Journal of Cosmetics, Dermatological Sciences and Applications*, **13**, 165-178.
https://doi.org/10.4236/jcdsa.2023.133015

Received: July 1, 2023
Accepted: September 4, 2023
Published: September 7, 2023

Abstract

Objective: Hemp seed oil is perfect for most skin types; it moisturizes skin and protects it from inflammation, oxidation, and other causes of aging. The problem is that the Hemp oil-based products do not penetrate the skin; they remain on the skin's surface. Recently researchers have been trying to prepare nano emulsions of hemp oil to facilitate its permeation to deep skin layers. In all techniques used today, surfactants are added to the emulsification process. These surfactants may cause unwanted skin side effects. In the present study, we prepare micronized Hemp (m-Hemp) without using any surfactants in the micronization process, thus avoiding the side effects associated with surfactant addition. Methods & Results: Particles size of m-Hemp was evaluated using electron microscopy. Various sizes of m-Hemp were found, the smallest being 100 nm in diameter. The antioxidation properties of m-Hemp were measured using the Electron Spin Resonance (ESR) technique and were found to be enhanced. Skin topography and morphology following a cream containing m-Hemp treatment were visualized by Optical Profilometry and ESEM respectively. The results show a marked improvement in skin topography in all measured parameters. In addition, human keratinocytes (HaCaT) were exposed to inflammatory conditions and were then treated using Hemp. As a result, one of the key inflammatory factors (IL-2) was significantly reduced after treatment with m-Hemp ($p \leq 0.0001$). The skin penetration of the cream containing m-Hemp was tested on human skin using the IMOPE (Iterative Multi-plane Optical Property Extraction) system. The results indicate that m-Hemp penetrates both the stratum corneum and the deep epidermal layers towards the dermis. Conclusion: The new cream pre-

pared with micronized Hemp shows significant anti-inflammatory and antioxidative effects and demonstrates the entrance of m-Hemp to the skin epidermal layer.

Keywords

Hemp, Microparticles, Anti-Inflammatory, Antioxidant, Skin Penetration

1. Introduction

Hemp seed oil (Hemp oil), obtained from the seeds of *Cannabis sativa* is known for its nutritive, health-enhancing properties and bioactivity. Hemp oil contains essential fatty acids (EFAs): Omega-6 fatty acids including linoleic acid, omega-3 containing the anti-inflammatory gamma linoleic acid (GLA) and omega 9. The ratio of omega-3 and omega-6, which are present in Hemp oil, is in the preferred ratio of 1:3 [1] for medical applications. Indeed recently Hemp oil has been found to exert antioxidative [2] [3] [4], and anti-inflammatory [5] [6] effects.

As to skin health, Hemp oil with the abundance of its fatty acids is an excellent choice for nourishing the skin and protecting it from inflammation, oxidation, and other causes of aging [7] [8]. Hemp oil does not contain tetrahydrocannabinol (THC), which is the psychoactive component of marijuana.

Hemp oil is extremely noncomedogenic, it can moisturize the pores without clogging them, and can help to balance out oily skin, hydrating it and regulating the skin's oil production. The gamma-linolenic acid component of the Hemp oil acts as a powerful anti-inflammatory agent [8] it hydrates the skin and treats cutaneous disorders resulting from skin ageing [9].

Hemp oil has been claimed to be useful for treating eczema and other skin diseases like dermatitis, seborrhoeic dermatitis/cradle cap, psoriasis and acne rosacea [10]. Unfortunately, there are not enough clinical studies proving it.

The problem is that the Hemp oil-based products do not penetrate the skin; they accumulate in the stratum corneum or remain on the skin surface. In order to treat inflammation, for example, Hemp oil has to conquer the skin barrier and reach inner layers.

Over the past decade, the research focus has been on preparing nano emulsions through various methods, broadly classified into two primary categories: high-energy and low-energy methods [11]. The downside of all these highly complex manufacturing procedures preparing nanoemulsions is the addition of surfactants to the emulsification system. During the process of decreasing the Hemp oil droplets to nano sizes, the surfactants themselves decrease to nano sized particles that might enter the skin barrier and cause unwanted side effects.

Surfactants are capable of interacting both with proteins and lipids in the stratum corneum, causing skin irritation. By penetrating through this layer, surfactants are also able to affect living cells in deeper regions of the skin. Further skin penetration may result in damage to cell membranes and structural com-

ponents of keratinocytes [12] [13] [14].

In the present research work supported by Hava Zingboim LTD, we have succeeded to produce micronized Hemp (m-Hemp) in a cream for topical use. In our technology there is no need to add any surfactants while preparing the micronized Hemp, so we avoid the side effects associated with high level surfactants. The micronized Hemp particles can penetrate the skin, have a high interfacial surface area and are stable. We have also been able to prove experimentally that the micronized Hemp formulated in a cream penetrates skin tissue.

In the present research work, the properties of our micronized Hemp are discussed. Particles obtained were characterized by scanning electron microscopy (SEM). The antioxidation properties of micronized Hemp were evaluated using Electron spin resonance (ESR) analysis. The anti-inflammatory effect of m-Hemp and Hemp oil were evaluated on human keratinocytes (HaCaT), a cell line broadly used in dermatological research [15] [16] [17] [18]. To induce inflammatory stress, the cells were treated with LPS [19] and the amount of IL-2, a key inflammatory factor in the skin, was measured [20] [21]. Hemp penetration depth in human skin was monitored using a new noninvasive optical technique called IMOPE (Iterative Multi-plane Optical Property Extraction) [22]. Optical profilometry was conducted for evaluating skin topography and roughness. Nile red staining was used for visulaziation of lipid droplets in skin tissue.

To the best of our knowledge, we are the first to measure penetration of Hemp while it is inserted in a cream.

2. Materials and Methods

2.1. Preparation of a New m-Hemp Cream

The newly prepared m-Hemp was inserted (2%) to a cream: Aqua (Water), Cetyl Alcohol, Silybum Marianum Ethyl Ester, Isoamyl Laurate, Hydrogenated Soybean Oil, Steareth-21, Cetearyl Ethylhexanoate, Castor Isostearate Succinate, Theobroma Cacao (Cocoa) Seed Butter, Hydroxyethyl Urea, Steareth-2, Sodium PCA, Sodium Lactate, Fructose, Glycine, Niacinamide, Urea, Inositol, Tocopherol, 1,2-Hexanediol, Dimethicone, Caprylyl Glycol, Xanthan Gum, Polyacrylate Crosspolymer-6, Trisodium Ethylenediamine Disuccinate, Magnolia Officinalis Bark Extract, Ethylhexylglycerin, Fragrance, Phenoxyethanol.

2.2. Determination of Hemp Size

Environmental Scanning Electron Microscope (ESEM) was used to determine m-Hemp size. Dynamic light scattering (DLS) was used for size and ζ potential measurements.

2.2.1. E-SEM

ESEM, FEI QUANTA-FEG250, was used for assessing the size of Hemp oil and m-Hemp. Particles solution was dried on round coverslips (13 mm) and coated with iridium (Q150T ES, Quorom technologies, England) prior to viewing.

2.2.2. DLS

The hydrodynamic radius and ζ potential of the samples were measured in particle analyzer, DLS (Malvern, Zetasizer, Nano-ZS).

2.3. Determination of Anti-Oxidative Capability of Hemp Oil Using Electron Spin Resonance (ESR) Spectroscopy

ESR is a very sensitive technique for determining Reactive Oxygen Species (ROS) like hydroxyl radicals for example.

In the present study, hydroxyl radicals were generated by performing a Fenton reaction ($Fe^{2+} + H_2O_2 \rightarrow Fe^{3+} + OH^* + OH^-$).

Since hydroxyl radicals have a very short half-life (ns-ms), making them very difficult to detect directly, there is a need to add a spin trap which bounds the hydroxyl radicals, to give a long-lived free radical, called a spin adduct, that can be detected by the ESR technique.

We used 5,5 dimethyl-1-pyrroline-N-oxide (DMPO) to trap hydroxyl radicals to yield DMPO-OH that has a quartet signal in the ESR spectrum. **Figure 1** shows a typical ESR spectrum of DMPO-OH adduct which is characterized by its 1:2:2:1 quartet of lines and hyperfine splitting constant aN and aH = 14.9. The area under the quartet signal is proportional to the amount of the hydroxyl radicals.

The anti-oxidative properties of m-Hemp relatively to those of Hemp oil were measured by the reduction of hydroxyl radicals generated in a Fenton reaction in the presence of m-Hemp or Hemp oil.

When the Fenton reaction is performed in the presence of Hemp oil/ m-Hemp, there is a decrease in the quartet signal, which indicates its anti-oxidative activity.

The effect of Hemp on the formation of hydroxyl radicals was investigated by adding it to a Fenton reaction system (H_2O_2 + $FeCl_2$ + DMPO + ddH_2O/Hemp oil/m-Hemp), and measuring the amount of hydroxyl radical produced via the Fenton reaction before and after the addition of Hemp /m-Hemp. The measured 100 µL aqueous suspensions mixture contained H_2O_2 (4400 µM, 10 µL) + $FeSO_4$ (500 uM, 10 µL) DMPO + DDW/Hemp/m-Hemp (10 µL) + MES Buffer pH = 6 (65 µL) + DMPO (5 µL). The mixture solution was introduced into a capillary micropipette (BRAND GMBH, Germany) and placed in a standard rectangular Bruker ESR cavity (ER 4119 HS) of Bruker ELEXSYSE500cw X-band ESR spectrometer. Room temperature spectra were acquired at a microwave frequency of 9.8 GHz, microwave power of 20 mW and Sweep width of 100 G (centered at 3518 G) with a modulation amplitude of 1G.

2.4. Determination of Anti-Inflammatory Capability of Hemp Oil Using ELISA Identification and Quantification of IL-2

HaCat cells were maintained in DMEM glucose (25.0 mM) with 10% FCS, 1% Pen-Strep, and 1% L-Glut. They were incubated at (37˚C) under 5% CO_2 atmosphere. The cells were allowed to grow for 24 h, then medium was refreshed

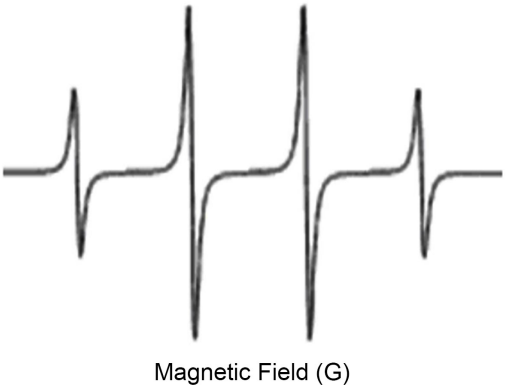

Figure 1. Typical DMPO-OH ESR Spectrum.

and cells were challanged with LPS from E. coli (O111:B4 Sigma Aldrich, Rehovot, Israel), at a concentration of 2 μg/ml for 30 min before the addition of m-Hemp/Hemp oil at concentrations of 5 and 10 μg/ml for a total of 24 h. At the end of incubation, the medium was taken for ELISA identification and quantification of IL-2 in the supernatant. ELISA testing (SYNERGY H1, Winooski, VT, United States) was conducted according to the manufacture's protocol (Biolegend, Legend MaxTM Human IL-2 ELISA kit). Statistical significance was assessed between groups, using a two-tailed Student's t test. Significance is set at $P < 0.05$.

2.5. Skin Specimens Processing and Preparation for Fluorescence Microscopy and Profilometry

Fresh human skin samples obtained by "Data-Biotech" (Rehovot 76701, Israel) were fixed in 10% buffered formalin and washed in sodium phosphate buffer at pH 7.2. Following overnight fixation, subcutaneous fat was partially reduced. Samples were cut leaving safety margins of 1 cm between each investigational site and the border of the tissue. For visualization samples were glued to round microscope cover slip (**Figure 2**).

Samples were washed using PBS at 37˚C (Biological Industries, 02-023-1A) 3 times (5 minutes each) and were primarily fixed with Karnovsky Fixative buffer consisting of 2.5% (wt/vol) paraformaldehyde (PFA), 2.5% glutaraldehyde, and 0.1M cacodylate buffer (EMC, 15949) for 1 h at room temperature and then left overnight at 4˚C.

The samples were dehydrated in a series of graded ethanol solutions (30%, 50%, 70%, and 95% and three times at 100%), for 10 min each, and then dried by vacuum (critical point drying-CPD).

CPD was performed using a Leica automatic EM CPD300 for 32 runs, with a cooling temperature of 7˚C, a heating temperature of 40˚C, stirrer speed set to 100%, and 100% advanced slow gas out.

Skin topography and morphology were visualized by Optical Profilometry and ESEM respectively.

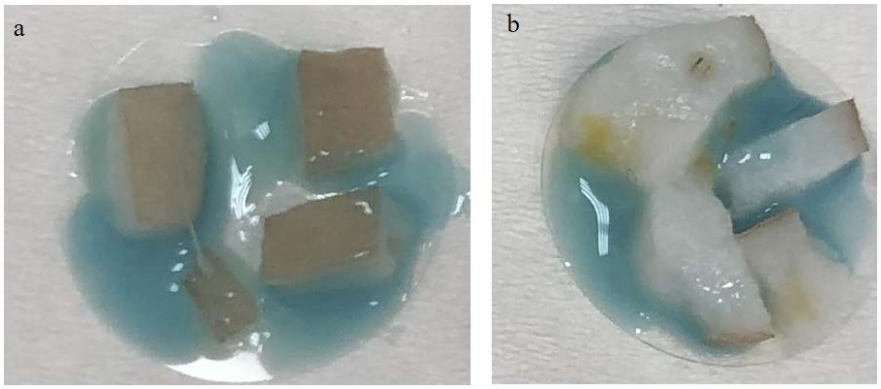

Figure 2. Skin specimen's preparation for (a) optical profilometry and (b) light microscopy coupled with Nile red staining.

2.6. Evaluation of Skin Topography

Optical profilometry was conducted for evaluating skin topography and roughness. It was performed on wet skin after initial overnight fixation in 10% PFA solution (**Figure 2(a)**) using 3D Measuring Laser Microscope (Olympus LEXT OLS4100, Japan), allowing a noncontact measuring of microstructure surface. In order to do a comparative study of skin topography and roughness, the arithmetical mean roughness (Sa), arithmetical difference between the highest and the lowest points (Sz) and Root mean squared roughness (Sq) were calculated. The (Sp) maximum peak height and (Sv) maximum valley depth were measured.

2.7. Tissue Staining with Nile Red

A 500 µg/ml stock Nile Red (Sigma-Aldrich) solution was prepared in acetone. Before use, the stock solution was diluted 1/100 in PBS (working solution). Skin tissue was soaked in the working solution in the dark for 30 min at 25˚C. Skin sample were rinsed 5 times with PBS for 5 min. Images were acquired on a Leica LMD7 upright microscope, driven by the LasX software. Fluorescent images were acquired using a standard red channel filter set.

Total image intensity in a specific region, reflecting depth of dye penetration, was measured by Cell Profiler software [23]. The region of interest (ROI) was of the same size in all images.

2.8. Skin Penetration of m-Hemp Cream Formulation

The skin penetration of m-Hemp in a cream was determined using the IMOPE system. The IMOPE technique [22] [24]-[28] is based on light propagation through a diffuser substance, like skin for example. Since the optical properties of the light parameters are affected by the structure of the skin, they can monitor the presence of different particles within the skin layers.

2.9. Skin Samples Preparation for IMOPE Experimental Setup

Fresh human skin samples obtained by "Data-Biotech" (Rehovot 76701, Israel) were examined macroscopically and microscopically to be intact without dam-

age scars. Skin areas of 2 cm^2 were treated in whole. Each cream sample (0.2 gr) was applied and speeded gently by cotton swab. During treatment, skin samples were placed on top of moist fabric in 3.5 cm petri-dishes. The skin was kept with the applied cream for 3 h.

The experiments were conducted using the IMOPE experimental setup for recording light intensity images at different locations along the Z axis as presented in Figure 3. The experimental setup is composed of a laser with a wavelength of μ = 633 nm, which is preferable for biomedical application. The other components within the setup are a lens, polarizers and a CMOS camera (Thor-Labs, New Jersey, US). The lens is used to focus the light beam, the polarizers for optical clearing purposes and the CMOS camera for recording the light intensity images. The skin samples set on a three-axis micrometer stage for adjustments in the x-y-z directions. For each sample, three points were measured, the reflected phase was reconstructed and its distribution, specifically the root mean square (RMS), was calculated using the IMOPE technique. The phase RMS was computed from a circular area with a radius size according to the tissue layer we were looking for. For each tissue sample, we examined the computed RMS before applying the cream (0 h) and 3 hours after (3 h). Since there is no real difference between the skin samples before applying the different creams, we calculated the average phase RMS at (0 h) from all samples together.

In order to examine the penetration depth of the Hemp, we conducted depth-scanning analysis. In the depth scanning the phase RMS is computed along the Z axis. The phase RMS of each sample was computed using the same algorithm parameters, a reconstruction thickness of 1.9 mm, and a distance between planes of 635 μm. The reconstruction was done along the Z axis, starting before the sample and advancing through the surface into the deeper layers.

In order to analyze the IMOPE results, we first conducted a literature search for optical properties of pig abdominal skin layers and their thicknesses [29]. The skin tissue was divided to two layers: SC (0.02 mm) and epidermis (0.1 mm). For each tissue layer the phase RMS is calculated from a specific circular area in accordance with the tissue's scattering.

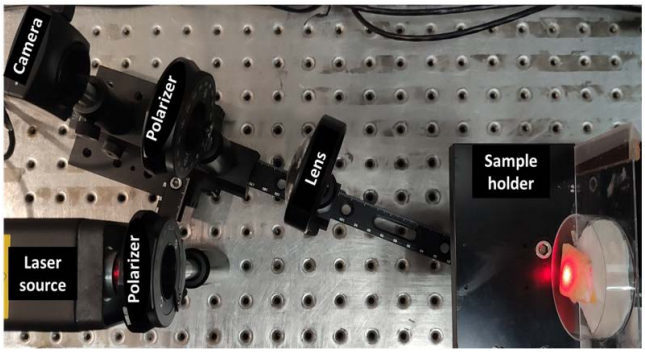

Figure 3. The experimental setup composed of a laser, polarizers for optical clearing purposes, a lens to focus the laser beam and a camera for recording light intensity images. The lens-polarizer-camera assembly sits on a stage which enables recording images at different depths.

By this method, in one phase image in a specific scan, we can analyze different layers in different depths.

The main advantage of the IMOPE technique is its ability to obtain data of different depths without the need of collecting separate samples (such as several skin biopsies). Moreover, this technique is in fact able to detect particles *in vivo* [27], thus, illiminating completely the need for biopsy collection.

3. Results and Discussion

3.1. Hemp Size and ζ Potential

Our micronizing technology led to a marked reduction in Hemp oil size. Since we don't add any surfactants to the system, we avoid the downsides associated with high level surfactants. The reduced sizes were evaluated using DLS and electron microscopy techniques. The hydrodynamic radius as measured by DLS was 434 ± 32 nm (75%) and 113 ± 12 (25%) for Hemp oil and m-Hemp respectively, (polydispersity index (PDI) 0.959 ± 0.04).

Particle stability in solution was assessed using ζ potential measurements.

High ζ potential, either positive or negative, is generally required to ensure stability. At large, systems with ζ potential > ± 30 mV are considered pharmaceutically stable [30].

The ζ of Hemp oil solution was measured at −31.93 ± 6.17 mV, while the ζ potential of m-Hemp increased to −42.9 ± 6.34 mV.

ESEM images of Hemp oil showed (**Figure 4**) irregular shaped aggregates (~ 1μ, inset **Figure 4(a)**) or large particles (**Figure 4(a)**). The m-Hemp obtained was markedly smaller with varied sizes ranging from 120 - 400 nm (**Figure 4(b)**).

Antioxidant Activity.

A marked increase in the antioxidant activity of m-Hemp (**Figure 5**) compared to Hemp oil was observed. A 70% reduction in the intensity of OH radicals was observed following addition of m-Hemp (**Figure 5(c)**), as compared to no-change (5% reduction) with Hemp oil (**Figure 5(b)**).

3.2. Anti-Inflammatory Effect of m-Hemp and Hemp Oil

HaCaT cells were treated with LPS (2 μg/ml) to induce inflammatory effect and then m-Hemp/Hemp oil was introduced to the cell medium for a total of 24 h.

As shown in **Figure 6**, m-Hemp at 5 μg/ml significantly (*) reduced IL-2 secretion by a factor of 5. Interestingly, Hemp oil showed slightly pro-inflammatory effect at all tested concentrations.

Skin topography measurements following m-Hemp cream treatment.

Profilometric data were obtained from analysis of skin samples treated with either the test formulation (base cream with m-Hemp) or control (base cream with Hemp oil) at ×5 and ×20 magnifications. The results for the topographical data (at ×5 magnification) are summarized in **Table 1**. The results show a marked improvement in skin topography in all parameters. The arithmetical difference between the highest and the lowest points (Sz) value was more than twice (2.38) lower in the treated skin sample. Finally, the mean roughness (Sa)

value in the m-Hemp treated skin (3.95) was 36% lower than in the Hemp oil treated one (6.138).

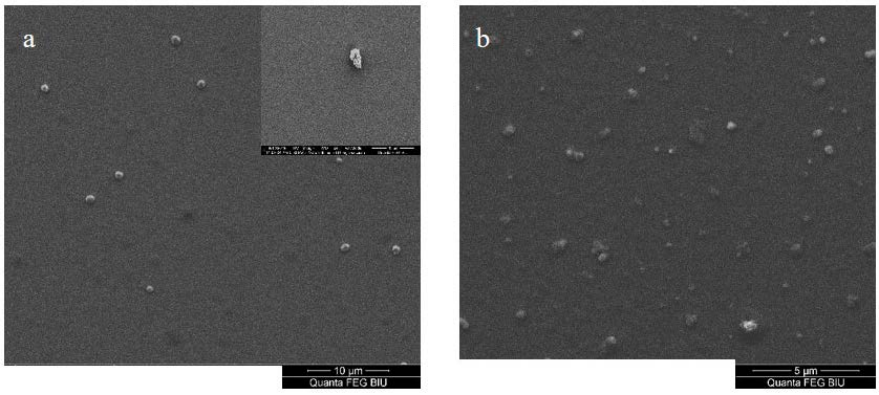

Figure 4. (a) Scanning electron microscopy image of Hemp oil (b) Scanning electron microscopy image of the m-Hemp.

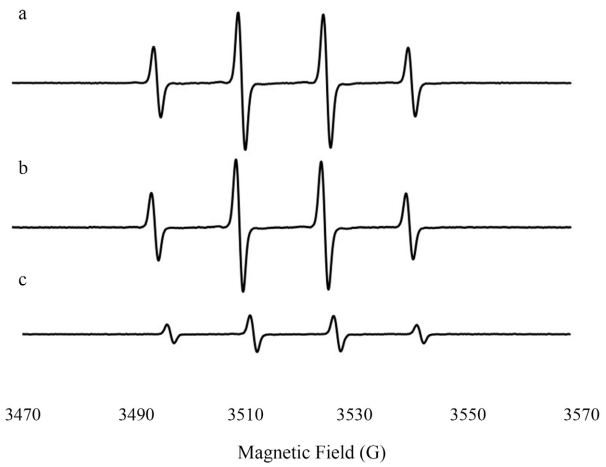

Figure 5. ROS formation: (a) Fenton, (b) Hemp oil, (c) m-Hemp.

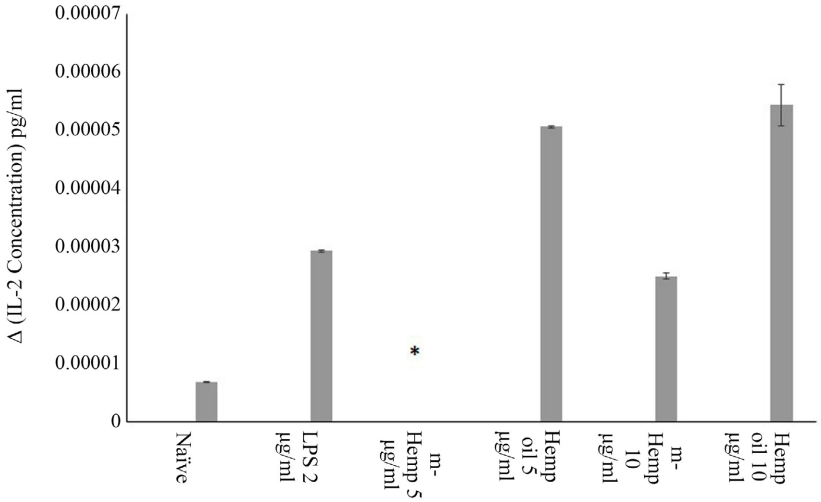

Figure 6. Effect of m-Hemp/Hemp oil on the levels of IL-2 in HaCat cell medium under LPS stimulation. The results presented as MEAN ± SE, $p \leq 0.0001$, $n = 4$.

3.3. Nile Red Staining

Total lipid content was visualized by staining the tissue with Nile red (9- diethylamino-5H-benzo [α]phenoxazine-5-one), Nile red is an excellent stain for the detection of lipids by fluorescence microscopy. For comparing lipid content in skin tissue two random areas (bearing the same distance from the upper layer of the skin sample) were chosen.

The Nile red stained skin samples demonstrated bright red (**Figure 7(a)**) and yellowish-gold (**Figure 7(b)**) fluorescence throughout the scanned areas of skin sample treated with Hemp oil cream or m-Hemp cream respectively. Mean Intensity of the fluorescence signal in the ROIs was calculated by the Cell Profiler software to be 0.268 a.u in the m-Hemp sample and 0.103 a.u in the Hemp oil treated sample. The increase in the lipid content in the m-Hemp sample points out that the m-Hemp penetrates the skin better than the Hemp oil.

3.4. Hemp Skin Penetration

The penetration of Hemp oil/m-Hemp to the skin layers was monitored by the IMOPE technique. As explained above, the IMOPE relates to the presence of particles with the phase RMS computed for the different layers. Following the analysis of the IMOPE technique, the change in the phase RMS which is proportional to the amount of detected particles in the various skin layers, is monitored for the cream containing Hemp oil/m-Hemp. See **Figure 8**. Note that the phase RMS contains the information about the base cream together with the hosted materials. Hence, in order to isolate the RMS base cream a threshold was set (dashed line in **Figure 8**). Using the threshold, we can evaluate only the presence of Hemp oil (**Figure 8(a)**) and m-Hemp (**Figure 8(b)**). Hemp oil and m-Hemp in the SC is monitored by blue lines and in the epidermis by orange lines. Note, only curves above the threshold line indicate the presence of Hemp oil and m-Hemp in the depth of the SC and epidermis.

Table 1. Topographical data.

	Sp (μm)	Sv (μm)	Sz (μm)	Sq (μm)	Sa (μm)
Tested formulation	34.815	39.034	73.848	5.351	3.95
Control	86.231	87.798	174.030	9.208	6.138

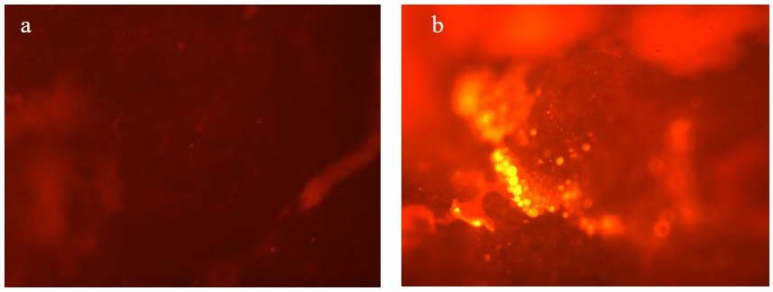

Figure 7. Nile red staining images of skin treated with (a) Hemp oil cream or (b) m-Hemp cream.

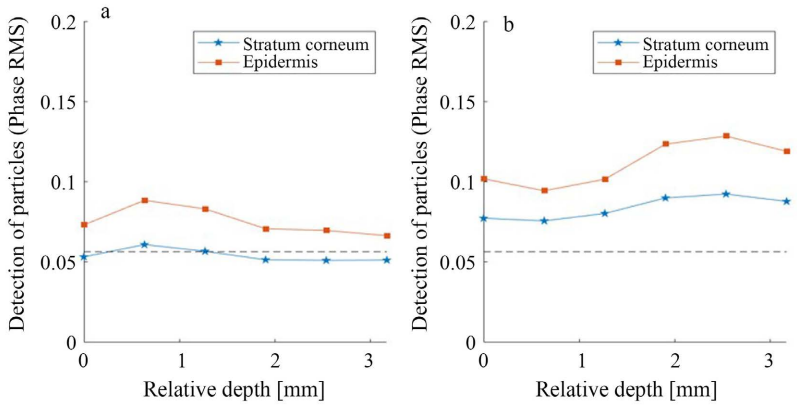

Figure 8. Phase RMS difference before and after applying cream with (a) Hemp oil and (b) m-Hemp. For each skin sample the change in the RMS, following the cream application, was computed for stratum corneum-SC (blue lines) and epidermis (orange lines). The black dashed line represents the threshold for detection of particles.

It can be observed that the Hemp oil (**Figure 8(a)**) 3 h after applying the skin, remains mostly around the threshold line which indicates its presence mostly on the skin surface. The m-Hemp (**Figure 8(b)**), however, exists in both layers where it increases mostly in the deep epidermis layer. We can conclude that following 3 h treatment the m-Hemp reaches the epidermis layer whereas the Hemp oil remains mostly on the skin surface.

4. Summary

Hemp seed oil is perfect for most skin types, it moisturizes skin and protects it from inflammation, oxidation, and other causes of aging. Unfortunately, it cannot enter deep skin layers. Many industries prepare micro emulsions of hemp oil but in their micronization process they use high amounts of surfactants, having serious side effects on skin. Our new facial cream contains m-Hemp made in a technique that does not involve surfactants in the process of micronization. The new m-Hemp cream has been proven to permeate the epidermis. In addition, significant antioxidative and anti-infammatory effects were also observed.

Hava Zingboim LTD will manufacture and deliver products containing micro Hemp prepared by her "Deep Skin Technology".

Acknowledgements

The authors would like to thank: Dr. Ronit Lavi, Dr. Avi Jacob and Mark Oksman for their assistance with ESR and microscopic measurements.

Conflicts of Interest

The authors declare no conflicts of interest regarding the publication of this paper.

References

[1] Hazekamp, A., Fischedick, J.T., Díez, L., Lubbe, A. and Ruhaak, R L. (2010) Chemi-

stry of Cannabis. In: Liu, H.-W. and Mander, L., Eds., *Comprehensive Natural Products II.*, Elsevier, Oxford, 1033-1084.

[2] Vitorović J., Joković, N., Radulović, N., Mihajilov-Krstev, T., Cvetković, V.J., Jovanović, N., Mitrović, T., Aleksić, A., Stanković, N. and Bernstein, N. (2021) Antioxidant Activity of Hemp (*Cannabis sativa* L.) Seed Oil in *Drosophila melanogaster* Larvae under Non-Stress and H_2O_2-Induced Oxidative Stress Conditions. *Antioxidants*, **10**, Article 830. https://doi.org/10.3390/antiox10060830

[3] Smeriglio, A., Galati, E.M., Monforte, M.T., Lanuzza, F., D'Angelo, V. and Circosta, C. (2016) Polyphenolic Compounds and Antioxidant Activity of Cold-Pressed Seed Oil from Finola Cultivar of *Cannabis sativa* L. *Phytotherapy Research*, **30**, 1298-1307. https://doi.org/10.1002/ptr.5623

[4] Sapino, S., Carlotti, M.E., Peira, E. and Gallarate, M. (2005) Hemp-Seed and Olive Oils: Their Stability against Oxidation and Use in O/W Emulsions. *Journal of Cosmetic Science*, **56**, 227-251.

[5] Rezapour-Firouzi, S., Mohammadian, M., Sadeghzadeh, M., Mehranfar, S. and Mazloomi, E. (2020) The Effects of Evening Primrose/Hemp Seed Oil Compared to Rapamycin on the Gene Expression of Immunological Parameters in Experimental Autoimmune Encephalomyelitis Splenocytes. *The Iranian Journal of Allergy, Asthma and Immunology*, **19**, 183-192.

[6] Jin, S. and Lee, M.Y. (2018) The Ameliorative Effect of Hemp Seed Hexane Extracts on the *Propionibacterium Acnes-Induced* Inflammation and Lipogenesis in Sebocytes. *PLOS One*, **13**, e0202933. https://doi.org/10.1371/journal.pone.0202933

[7] Vaughn, A.R., Clark, A.K., Sivamani, R.K. and Shi, V.Y. (2018) Natural Oils for Skin-Barrier Repair: Ancient Compounds Now Backed by Modern Science. *American Journal of Clinical Dermatology*, **19**, 103-117. https://doi.org/10.1007/s40257-017-0301-1

[8] Kapoor, R. and Huang, Y.S. (2006) Gamma Linolenic Acid: An Anti-Inflammatory Omega-6 Fatty Acid. *Current Pharmaceutical Biotechnology*, **7**, 531-534. https://doi.org/10.2174/138920106779116874

[9] Costedoat, M.R.S. and Wepierre, J. (1981) Percutaneous Absorption and Distribution of (14) C-Gamma-Linolenic Acid in Hairless Rats and Man. *International Journal of Cosmetic Science*, **3**, 83-93.

[10] Tabassum, N. and Hamdani, M. (2014) Plants Used to Treat Skin Diseases. *Pharmacognosy Reviews*, **8**, 52-60. https://doi.org/10.4103/0973-7847.125531

[11] Fryd, M.M. and Mason, T.G. (2012) Advanced Nanoemulsions. *The Annual Review of Physical Chemistry*, **63**, 493-518. https://doi.org/10.1146/annurev-physchem-032210-103436

[12] Badmus, S.O., Amusa, H.K., Oyehan, T.A. and Saleh T.A. (2021) Environmental Risks and Toxicity of Surfactants: Overview of Analysis, Assessment, and Remediation Techniques. *Environmental Science and Pollution Research*, **28**, 62085-62104. https://doi.org/10.1007/s11356-021-16483-w

[13] Yuan, C.L., Xu, Z.Z., Fan, M.X., Liu, H.Y., Xie, Y.H. and Zhu, T. (2014) Study on Characteristics and Harm of Surfactants. *Journal of Chemical and Pharmaceutical Research*, **6**, 2233-2237.

[14] Seweryn, A. (2018) Interactions between Surfactants and the Skin—Theory and Practice. *Advances in Colloid and Interface Science*, **256**, 242-255. https://doi.org/10.1016/j.cis.2018.04.002

[15] Kahremany, S., Hofmann, L., Eretz-Kdosha, N., Silberstein, E., Gruzman, A. and

Cohen, G. (2021) SH-29 and SK-119 Attenuates Air-Pollution Induced Damage by Activating Nrf2 in HaCaT Cells. *International Journal of Environmental Research and Public Health*, **18**, Article 12371. https://doi.org/10.3390/ijerph182312371

[16] Kahremany, S., Babaev, I., Gvirtz, R., Ogen-Stern, N., Azoulay-Ginsburg, S., Senderowitz, H., Cohen, G. and Gruzman, A. (2019) Nrf2 Activation by SK-119 Attenuates Oxidative Stress, UVB, and LPS-Induced Damage. *Skin Pharmacology and Physiology*, **32**, 173-181. https://doi.org/10.1159/000499432

[17] Li, C., Liu, W., Wang, F., Hayashi, T., Mizuno, K., Hattori, S., Fujisaki, H. and Ikejima, T. (2021) DNA Damage-Triggered Activation of cGAS-STING Pathway Induces Apoptosis in Human Keratinocyte HaCaT Cells. *Molecular Immunology*, **131**, 180-190. https://doi.org/10.1016/j.molimm.2020.12.037

[18] Blanchard, G., Pich, C. and Hohl, D (2020) HaCaT Cells As a Model System to Study Primary Cilia in Keratinocytes. *Experimental Dermatology*, **31**, 1276-1280.

[19] Wei, M., Liu, F., Raka, R., Xiang, J., Xiao, J., Han, T., Guo, F., Yang, S. and Wu. H. (2022) *In vitro* and *in silico* Analysis of "Taikong Blue" Lavender Essential Oil in LPS-Induced HaCaT Cells and RAW 264.7 Murine Macrophages. *BMC Complementary Medicine and Therapies*, **22**, Article No. 324. https://doi.org/10.1186/s12906-022-03800-0

[20] Lee, K.J., Ratih, K., Kim, G.J., Lee, Y.R., Shin, J.S., Chung, K.H., Choi, E.J., Kim, E.K. and An, J.H. (2022) Immunomodulatory and Anti-Inflammatory Efficacy of Hederagenin-Coated Maghemite (γ-Fe_2O_3) Nanoparticles in An Atopic Dermatitis Model. *Colloids and Surfaces B*: *Biointerfaces*, **210**, Article 112244. https://doi.org/10.1016/j.colsurfb.2021.112244

[21] Ying, Z., Li, X., Dang, H., Yin, N. and Gao, C. (2020) Molecular Immune Mechanisms of HPV-infected HaCaT Cells *in vitro* Based on Toll-Like Receptors Signaling Pathway. *Journal of Clinical Laboratory Analysis*, **34**, e23101. https://doi.org/10.1002/jcla.23101

[22] Yariv, I., Rahamim, Shliselberg, E.G., Duadi, H., Lipovsky, A., Lubart, R. and Fixler, D. (2014) Detecting Nanoparticles in Tissue Using An Optical Iterative Technique. *Biomedical Optics Express*, **5**, 3871-3881. https://doi.org/10.1364/BOE.5.003871

[23] Lamprecht, M.R., Sabatini, D.M. and Carpenter, A.E. (2007) Cell Profiler: Free, Versatile Software for Automated Biological Image Analysis. *Biotechniques*, **42**, 71-75. https://doi.org/10.2144/000112257

[24] Yariv, I., Haddad, M., Duadi, H., Motiei, M. and Fixlr, D. (2016) New Optical Sensing Technique of Tissue Viability and Blood Flow Based on Nanophotonic Iterative Multi-Plane Reflectance Measurements. *International Journal of Nanomedicine*, **11**, 5237-5244. https://doi.org/10.2147/IJN.S119130

[25] Yariv, I., Duadi, H., Chakraborty, R. and Fixler, D. (2019) Algorithm for *in vivo* Detection of Tissue Type from Multiple Scattering Light Phase Images. *Biomedical Optics Express*, **10**, 2909-2917. https://doi.org/10.1364/BOE.10.002909

[26] Yariv, I., Duadi, H. and Fixler, D. (2020) Depth Scattering Characterization of Multi-Layer Turbid Media Based on Iterative Multi-Plane Reflectance Measurements. *IEEE Photonics Journal*, **12**, Article 3700713. https://doi.org/10.1109/JPHOT.2020.3017697

[27] Yariv, I., Kannan, S., Harel, Y., Levy, E., Duadi, H., Lellouche, J.P., Michaeli, S. and Fixler, D. (2021) Iterative Optical Technique for Detecting Anti-Leishmania Nanoparticles in Mouse Lesions. *Biomedical Optics Express*, **12**, 4496-4509. https://doi.org/10.1364/BOE.425798

[28] Yariv, I., Duadi, H. and Fixler, D. (2019) An Optical Method to Detect Tissue Scat-

tering: Theory, Experiments and Biomedical Applications. *Proceedings of the SPIE*, **10891**, Article 1089105. https://doi.org/10.1117/12.2508335

[29] Bashkatov, A.N., Genina, E.A. and Tuchin, V.V. (2011) Optical Properties of Skin, Subcutaneous, and Muscle Tissues: A Review. *Journal of Innovative Optical Health Sciences*, **4**, 9-38. https://doi.org/10.1142/S1793545811001319

[30] Sharma, S., Shukla, P., Misra, A. and Mishra, P.R. (2014) Chapter8-Interfacial and Colloidal Properties of Emulsified Systems: Pharmaceutical and Biological Perspective. *Colloid Interface Science in Pharmaceutical Research and Development*, **2014**, 149-172. https://doi.org/10.1016/B978-0-444-62614-1.00008-9